Spectroscopic Characterization of CVD Ti Coating on SiC-Coated Boron Fibers

Beng Jit Tan,[†,‡] Luchen Hwan,[†] and Steven L. Suib*[,†,‡,§]

Department of Chemistry, U-60, University of Connecticut, Storrs, Connecticut 06269-3060; Institute of Materials Science, University of Connecticut, Storrs, Connecticut 06269; and Department of Chemical Engineering, University of Connecticut, Storrs, Connecticut 06269

Francis S. Galasso

United Technologies Research Center, East Hartford, Connecticut 06108

Received August 29, 1990. Revised Manuscript Received December 18, 1990

Auger electron and X-ray photoelectron spectroscopies were employed to investigate the fiber–matrix interface produced by the chemical vapor deposition of titanium on SICABO and BORSIC fibers at 1040 °C. Chemical state information about the titanium coating and the Ti/SiC interface was obtained. The chemical nature of the coating was observed through the behavior of the Si 2p, C 1s, and Ti 2p photoelectron core levels and their corresponding Si LVV, C KLL, Ti LMM, and Ti LMV Auger electron spectra. Sputter-depth profiling was employed to complete the characterization of the material formed by interfacial reaction. The Ti was found to react with the BORSIC fiber, forming large amounts of titanium silicides and titanium carbide, whereas only small amounts of titanium carbide and titanium silicides were formed with the SICABO fiber. Sputter-depth profiling reveals that growth of the titanium silicides and carbide takes place over considerable depth into the BORSIC fiber. The reaction zone in titanium-coated SICABO fiber was not as broad.

Introduction

The mechanical properties of fiber-reinforced materials are strongly dependent on the reaction between fiber and matrix. Fiber–matrix interfacial properties play an important role in determining the structural integrity of the composite. Fiber–matrix interfacial bonding is also a major factor in improving the fracture toughness of a fiber-reinforced ceramic. Studies have shown that a strong fiber–matrix bond is unfavorable as this leads to a brittle high-strength material. On the other hand, a weaker bond is desirable as this toughens the composite through energy-dissipative processes such as fiber pullout.[1] With a thorough understanding of the surface and interface properties in ceramic composites at various stages in their synthesis, it should be possible to formulate atomic level strategies for optimizing the final bulk product.

The present surface study of CVD titanium coatings on SiC-coated boron fibers was motivated by renewed interest in the formation of titanium matrix composites. Recently we reported that SICABO fiber is more stable than BORSIC (Hamilton Standard) fiber in titanium composites.[2] In particular, the tensile strength of the BORSIC fiber was severely degraded in the hot-pressed Ti matrix composites at the fabrication temperature of 930 °C. In contrast, the SICABO fibers retained their tensile strength after hot pressing. We also showed that CVD Ti-coated BORSIC fibers showed greater strength degradation than CVD Ti-coated SICABO fibers when subjected to post-deposition heat treatments in helium. The present study employs X-ray photoelectron spectroscopy and Auger electron spectroscopy to examine the surface of the as-received SiC-coated boron fibers as well as the chemical composition of the CVD Ti coating on these fibers. As presented in this paper, these measurements provide a basis for interpreting the composition of the Ti/SiC interface and, thus, ultimately for understanding the role played by interfaces in the bulk properties of these Ti-coated SICABO and BORSIC (Hamilton Standard) fibers.

Experimental Section

Materials. XPS and AES analyses of reference materials were performed to interpret Ti matrix–fiber interface analysis data. Pure Ti was obtained commercially from Johnson Matthey as a 1-mm-thick foil. SiC, TiC, TiO_2, Ti_5Si_3, and $TiSi_2$ powder standards were also obtained from Johnson Matthey. The identities of the reference compounds were verified by X-ray diffraction. $TiCl_4$ used in the Ti CVD synthesis was obtained from Alfa Products. Ultrapure grade hydrogen was bubbled through the $TiCl_4$ before use to remove dissolved gases. Ultrapure grade H_2 and He gases were obtained from Aero All Gas Co. The BORSIC fibers were obtained from Hamilton Standard, and the SICABO fibers were obtained from Composites Inc., Manchester, CT.

Titanium CVD Synthesis. Titanium was synthesized by reducing $TiCl_4$ in hydrogen at 1040 °C at atmospheric pressure. Details of the CVD procedure are described elsewhere.[2] The temperature of the furnace was slowly increased from room temperature to 1040 °C over 30 min. During this time the system was purged with ultrapure H_2. Once this temperature was reached, the H_2 gas was switched over to a $TiCl_4/H_2$ mixture. The ratio of H_2:$TiCl_4$ was 75:1. The hydrogen was used as a carrier gas as well as a reducing agent. The flow rate of the hydrogen gas was 75 mL min^{-1}. Deposition of the Ti was continued for 30 min, after which the $TiCl_4/H_2$ gas mixture was switched back to H_2 gas alone. By the end of this time a coating of about 1 μm thick would have been deposited (vide infra). The coated fibers were then allowed to cool to room temperature in H_2 gas flow for 3 h.

Apparatus. Photoelectron spectroscopy measurements were carried out using a Physical Electronics PHI 5300 X-ray photoelectron spectrometer, using monochromatic Al Kα X-radiation. The power was 600 W (15 keV, 40 mA). The base pressure in the sample chamber was 3×10^{-9} torr. The spectrometer is also equipped with an electron flood gun that provides a low flux of electrons to compensate for sample charging. Low-resolution broad scans were collected at a pass energy of 178.9 eV in order to survey elemental composition over the entire XPS energy range. High-resolution spectra were collected at a pass energy of 35.75

[†] Department of Chemistry.
[‡] Institute of Materials Science.
[§] Department of Chemical Engineering.
* To whom correspondence should be addressed.

(1) Homeny, J.; Vaughn, W. L. *Mater. Res. Soc. Bull.* **1987**, *12*, 66.
(2) Hwan, L.; Tan, B. J.; Suib, S. L.; Galasso, F. *Mater. Res. Soc. Symp. Proc.* **1990**, *168*, 239.

0897-4756/91/2803-0368$02.50/0

eV to obtain more detailed chemical information of the fiber surface. At this pass energy, the peak width for the Ag $3d_{5/2}$ line is 0.7 eV. The sample spot size is 2 mm × 10 mm. Calibration was based upon the C 1s photoelectron peak of adventitious carbon at 284.6 eV. For the O 1s, C 1s, Si 2p, and Ti 2p states of primary interest in this study, the photoelectron escape depths give spectral contributions from the top 20–30 Å of the sample material.[3]

The AES spectra were obtained with a Physical Electronics PHI 610 scanning Auger spectrometer with a base pressure of 5 × 10^{-9} Torr. The spectrometer is equipped with a single-pass cylindrical mirror analyzer (CMA) with a coaxial electron gun. Auger spectra were recorded with an energy resolution of 0.6%. Surface compositions were analyzed in the "as received" state and after different sputtering times at 3-keV primary electron energy and a 50-nA beam current. The spectral regions of interest include Ti LMM (320–460 eV), O KLL (460–540 eV), C KLL (220–300 eV), and Si LMM (40–120 eV).

Composition depth profiles of the near surface layers were obtained in both XPS and AES analysis. The spectra were collected after sputtering with a differentially pumped ion gun employing argon as the sputtering gas. A focused 3-keV ion beam rastered over a 10 mm × 10 mm area was used for sputtering in XPS studies. AES depth profiles were obtained by using a 3-keV Ar^+ ion beam rastered over an area of 2 mm × 2 mm. Under these conditions the AES sputtering rate for TiO_2 was 10 Å min^{-1}.

Sample Preparation for AES and XPS Analysis. The powder standards (SiC, TiC, TiO_2, Ti_5Si_3, and $TiSi_2$) were prepared for XPS analysis by dusting the powders onto double sided sticky tape (3M Co.). The particle sizes of the powder standards were in the same size range of 1–2 μm. In the case of AES analyses, the powders were pressed into an indium support. Care was taken to ensure that the powders completely covered the sticky tape and the indium support. The Ti foil was clipped to the sample block using a copper clip. Before data collection, the foil was argon-ion sputter cleaned in situ. Sample charging of the powder standards during XPS analysis was compensated for by employing a flood gun.

For XPS studies, 60–70 fibers of 1.3 cm in length were sandwiched between a copper mask with a window dimension of 10 mm × 10 mm and a sample block with a rectangular groove. This ensured that no signal from the sample block was detected once the fibers were aligned with the analyzer of the spectrometer. The copper mask was then clipped to a hollow sample block. For AES studies, a single fiber was sandwiched between a three-hole mask and a sample block with a rectangular groove. The mask was held in place by screws. The reason for using the masks in the XPS and AES experiments is to provide good electrical contact as well as to ensure that the fibers are held well in place.

Data Analysis. Analyses and manipulation of XPS and AES data were carried out using built-in software by Physical Electronics. XPS spectra were fitted by using a nonlinear least-squares method with a Gaussian/Lorentzian (G/L) peak shape after a nonlinear background was removed. A G/L mixing ratio of 90–100% was employed. Atomic percentage concentration of a given surface component was obtained from the integrated peak area of the individual components and employing the sensitivity factors provided by Physical Electronics.[4] The integrated peak area was obtained after subtraction of a nonlinear background.

The digitally stored AES data were differentiated numerically for quantification since the data were collected in the direct N(E) mode. The Auger peak-to-peak height (APPH) is used as a measure of sample composition. The APPHs were recorded for silicon (Si LVV, 92 eV), carbon (C KLL, 272 eV), titanium (Ti LMV, 383 eV), and oxygen (O KLL, 510 eV). The atomic percentage concentrations of the individual components were obtained from the APPHs and employing the sensitivity factors provided by United Technologies[5] and Physical Electronics.[6] The

(3) Seah, M. P.; Dench, W. A. *Surf. Interface Anal.* **1979**, *1*, 2.
(4) Wagner, C. D.; Riggs, W. H.; Davis, L. E.; Moulder, J. F.; Muilenberg, G. E. *Handbook of X-ray Photoelectron Spectroscopy*, 2nd ed.; Perkin-Elmer, Physcial Electronics Division: Eden Prairies, MN, 1979.
(5) Private communication with Dr. Bruce Laube, United Technologies Research Center, East Hartford, CT.
(6) Davis, L. E.; Mac Donald, N. C.; Palmberg, P. W.; Rinch, G. E.; Weber, R. W. *Handbook of Auger Electron Spectroscopy*, 2nd ed.; Perkin-Elmer, Physical Electronics Division: Eden Prairies, MN, 1979.

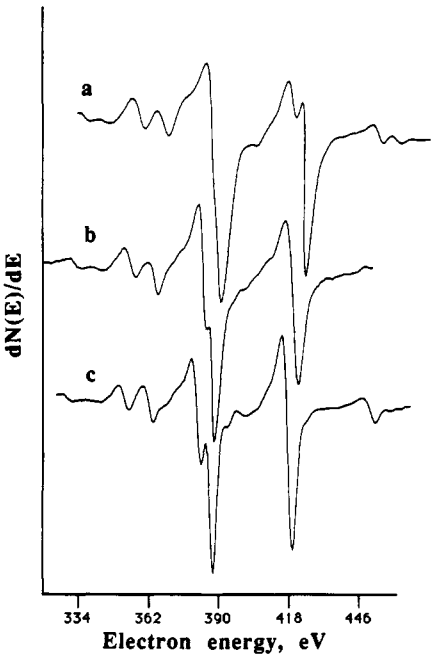

Figure 1. Auger Ti $L_3M_{2,3}M_{2,3}$ and $L_3M_{2,3}M_{4,5}$ line shapes for some reference materials: (a) titanium(IV) oxide; (b) titanium carbide, and (c) titanium silicide, Ti_5Si_3.

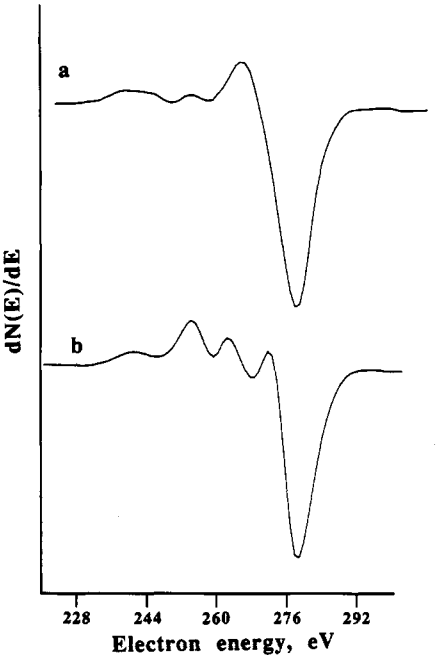

Figure 2. Auger C KLL line shapes for (a) silicon carbide and (b) titanium carbide.

AES depth profile results were obtained from the relative atomic percentage concentrations of Ti, O, C, and Si plotted as a function of sputter time.

Results

Reference Compounds. The Ti $L_{2,3}M_{2,3}M_{2,3}$ and $L_3M_{2,3}M_{4,5}$ Auger line shapes for bulk TiO_2, TiC, and Ti_5Si_3 are shown in Figure 1. Figure 2 compares the C KLL Auger line shapes of TiC and SiC. It is evident that there are sufficient differences in the Auger line shapes to allow for chemical state identification.

The photoelectron binding energies of the relevant Ti and Si reference compounds are listed in Table I, which are in agreement (±0.3 eV) with binding energies reported in the literature.[7-9] The XPS binding energies for these

Table I. Core Level Binding Energies[a] (electronvolts) for Various Reference Materials

sample	Ti $2p_{3/2}$	C 1s	O 1s	Si 2p
Ti foil	453.8 (1.1)			
TiC	455.2 (4.3)	281.8 (1.9)		
TiO_2	458.6 (4.5)		530.0 (2.0)	
$TiSi_2$	453.4 (4.5)			98.5 (1.9)
Ti_5Si_3	453.4 (4.5)			98.7 (1.9)
SiO_2			532.1 (2.0)	103.8 (2.1)
SiC		282.5 (1.9)		100.4 (1.9)

[a] Binding energies are with respect to C 1s of adventitious carbon at 284.6 eV and are reported with an accuracy of ±0.3 eV. [b] Values in parentheses are full width at half-maximum (fwhm) peak heights.

Table II. XPS Binding Energies (electronvolts)[a,b] for As-Received and Argon Ion Sputtered BORSIC and SICABO Fibers

sample	C 1s	O 1s	Si 2p
as-received BORSIC	286.4 (1.7), 284.6 (1.7), 282.8 (1.7)	531.8 (2.1)	102.6 (1.9), 100.3 (1.9)
etched BORSIC	—, 284.6 (1.7), 283.1 (1.7)	—	—, 100.3 (1.9)
as-received SICABO	286.3 (1.7), 284.6 (1.7), 282.9 (1.7)	532.0 (2.0)	102.5 (1.9), 100.4 (1.9)
etched SICABO	—, 284.6 (1.7), 283.2 (1.7)	—	—, 100.4 (1.9)

[a] Binding energies are with respect to C 1s of adventitious carbon at 284.6 eV. [b] Values in parentheses are full width at half-maximum (fwhm) peak heights.

series of reference compounds are useful models for species that may exist in the Ti–SiC–coated B fibers. The chemical shifts are large enough for XPS to distinguish between the various Ti and Si compounds of interest.

BORSIC and SICABO Fibers. (i) XPS results: Both BORSIC and SICABO fibers show strong Si 2p, O 1s, and C 1s peaks. The peak shapes and line positions of the regions of interest for both types of fibers are essentially similar to each other. Figure 3 shows the typical spectral line shapes for C 1s (Figure 3A) and Si 2p (Figure 3B) obtained for the BORSIC fiber before and after a light Ar^+ etch in order to remove surface contamination, and Table II summarizes the peak positions of the spectral regions of interest for the as-received BORSIC and SICABO fibers as well as those of the corresponding etched fibers.

A careful study of the high-solution XPS spectra reveals that the SiC coatings of the SICABO and BORSIC fibers are oxidized on the surface giving rise to SiO_2. The Si 2p region of the as-received BORSIC and SICABO fibers could not be separated into the spin–orbit components at the resolution employed and shows a major peak at 100.3 eV and a broad shoulder toward higher binding energy. The Si 2p peak at 100.3 eV compares favorably in binding energy with that of the SiC standard as well as values reported for cleaved polycrystalline SiC (100.2 eV)[10] and the (001) faces of single-crystal α-SiC (100.4 eV).[8,11] The broad shoulder centered at 102.6 eV is attributed to a mixture of suboxide states. Studies of reactively deposited silicon oxide films and thermally grown Si–SiO_2 interfaces have shown that there is a progression of suboxide states (1+, 2+, 3+ silicon valence designation) prior to the formation of stoichiometric SiO_2.[12-15] Taking the simplest

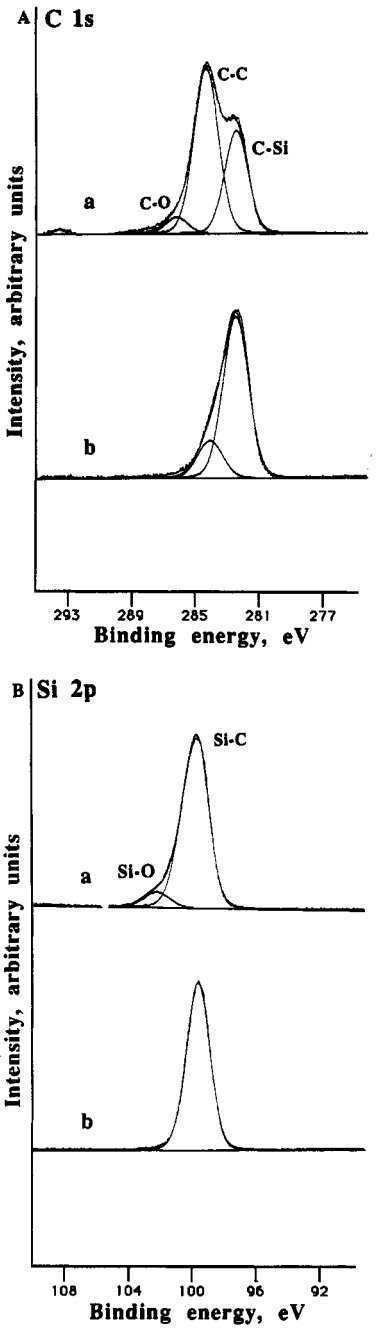

Figure 3. X-ray photoelectron spectral regions of the (A) C 1s and (B) Si 2p envelopes of the (a) as-received and (b) etched BORSIC fiber.

explanation[16,17] that each valence state contributes a 1.1-eV shift to higher binding energy from elemental silicon (Si 2p binding energy of 99.2 eV),[12,16,18] the broadening of the Si 2p envelope on the high-binding-energy side could correspond to silicon suboxide/oxide bonding. On etching, the surface oxide layer is removed, and the broad peak at higher binding energy is no longer observed.

The C 1s spectrum of the as-received fibers shows two strong peaks with binding energies of 284.6 and 282.8 eV

(7) Anthony, M. T.; Seah, M. P. *Surf. Interface Anal.* **1984**, *6*, 138.
(8) Miyoshi, K.; Buckley D. H. *Appl. Surf. Sci.* **1982**, *10*, 357.
(9) Wei, Y. Y.; et al. *Jpn. J. Appl. Phys.* **1984**, *23*, 1560.
(10) Smith, K. L.; Black, K. M. *J. Vac. Sci. Technol.* **1984**, *A2*, 744.
(11) Muehlhoff, L.; Choyke, W. J.; Bozack, M. J.; Yates, J. T. Jr. *J. Appl. Phys.* **1986**, *60*, 2842.
(12) Barr, T. L. *Appl. Surf. Sci.* **1983**, *15*, 1.
(13) Finster, J.; Schulze, D.; Meisel, A. *Surf. Sci.* **1985**, *162*, 671.
(14) O'Leary, M. J.; Thomas, J. H. *J. Vac. Sci. Technol.* **1983**, *A1*, 640.
(15) Hattori, T.; Suzuki, T. *Appl. Phys. Lett.* **1983**, *43*, 470.
(16) Raider, S. I.; Flitsch, R. *IBM J. Res. Develop.* **1978**, *22*, 294.
(17) Raider, S. I.; Flitsch, R. *J. Electrochem. Soc.* **1976**, *123*, 1754.
(18) Wagner, C. D.; Passoja, D. E.; Hillery, H. F.; Kinisky, T. G.; Six, H. A.; Jansen, W. T.; Taylor, J. A. *J. Vac. Sci. Technol.* **1982**, *21*, 933.

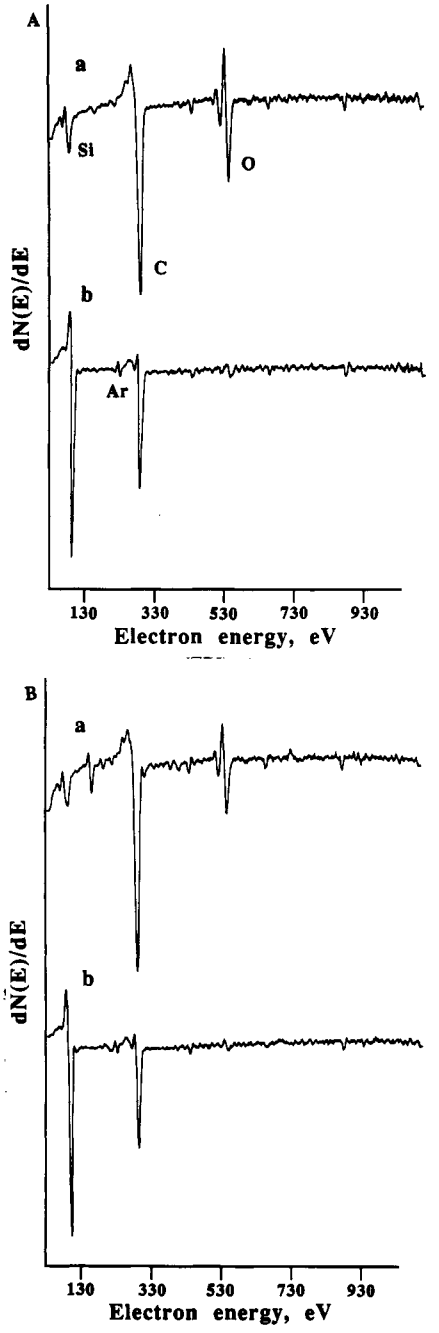

Figure 4. Survey Auger electron spectra of (A) BORSIC and (B) SICABO fiber in the (a) as-received state and (b) after 15-min argon ion etch.

that correspond to adventitious carbon and silicon carbide,[8,10,11] respectively. A third peak at 286.4 eV is attributed to C–O species from surface carbon contamination. Ar^+ etching removes the surface carbon contamination, and the peak intensity of the line at 284.6 eV decreases relative to that of SiC at 283.2 eV.

The charge-corrected O 1s binding energies are observed in a similar range of binding energies reported by Wagner and co-workers for silica-related material.[18,19]

(ii) AES results: Broad-scan spectra of the as-received and etched SICABO and BORSIC fibers are essentially similar, showing the presence of Si, C, and O (Figure 5). On argon ion etching, the surface hydrocarbon and adventitious carbon are removed and the surface of the fiber is exposed. In agreement with XPS results, the AES results also show that the surface is composed of a thin layer (150–200 Å thick) of silicon suboxides/oxide. Removal of this layer by argon ion sputtering causes a decrease in the relative intensity of the O peak to almost the noise level. The relative atomic concentration ratios for C/Si decrease from 7.4 to 1.0 and that of O/Si decreases from 1.9 to 0.0 when the SICABO fiber surface was argon ion sputtered cleaned. A similar decrease in these two ratios was observed in the case of sputter cleaned BORSIC fiber (C/Si from 12.8 to 1.0 and O/Si from 2.0 to 0.0). The changes in relative peak-to-peak heights are readily observed in survey scans (Figure 4).

Table III. Peak Percentage Areas for the C 1s Region of Ti-SICABO for the Argon Ion Etching Experiments

etch time, min	C–Ti (281.6)[a]	C–Si (282.5)	C–H (284.6)	C=O (285.4)	C–O (288.4)
0	0.0[b]	0.0	71.8	17.7	10.5
25	24.8	0.0	63.8	11.4	0.0
85	9.9	36.3	47.3	6.6	0.0
140	6.7	57.2	30.6	5.6	0.0

[a] Value in parentheses is the binding energy (electronvolts) of the peak corresponding to the carbon species denoted above it. [b] Percentage area of the peak.

Table IV. Peak Percentage Areas for the C 1s Region of Ti-BORSIC for the Argon Ion Etching Experiments

etch time, min	C–Ti (281.6)[a]	C–Si (282.5)	C–H (284.6)	C=O (285.4)	C–O (288.4)
0	2.9[b]	0.0	69.0	21.1	7.0
25	12.2	0.0	72.4	11.1	4.3
85	12.8	6.2	73.6	7.5	0.0
140	29.3	10.2	52.8	7.7	0.0

[a] Value in parentheses is the binding energy (electronvolts) of the peak corresponding to the carbon species denoted above it. [b] Percentage area of the peak.

Thus from XPS and AES results one can conclude that the surfaces of the SICABO and BORSIC fibers are composed of an overlayer of adventitious carbon- and hydrocarbon-containing surface impurities beneath which is a thin layer (150–200 Å thick) of silicon oxides/suboxides.

CVD Titanium-Coated SICABO and BORSIC Fibers. (i) XPS results: The XPS results show that the surfaces of both the Ti-coated SICABO (Ti-SICABO) fibers and Ti-coated BORSIC (Ti-BORSIC) fibers are covered by a layer of adventitious carbon and the Ti coatings are rich in surface TiO_2 (Figure 5IA and 5IIA for Ti-SICABO and Ti-BORSIC, respectively). The Ti $2p_{3/2}$ peak at 458.7 eV is characteristic of TiO_2. The corresponding O 1s envelopes for both coated fibers, which are not shown, consist of three peaks centered at 530.1, 531.4, and 532.2 eV. The O 1s peak at 530.1 eV corresponds to oxygen bonded to TiO_2, and the other two peaks at higher binding energy are due to oxygen present in the form of adsorbed water and hydroxyl groups, respectively. The C 1s envelope of both coated fibers (Figure 5IB and 5IIB) show chemical states assigned to adventitious carbon (284.6 eV) and small amounts of carbon bonded to oxygen.[20] In addition to these carbon species, the surfaces of Ti-BORSIC fibers also show the presence of TiC as evidenced by the C 1s peak centered at 281.7 eV.[21] TiC is not observed on the surface of Ti-SICABO fibers.

The C 1s spectrum shows that TiC (C 1s = 251.6 eV) is present within the bulk of the coating in both fibers. The TiC peak in Ti-BORSIC has a relatively high peak intensity among all carbon species present. The changes

(19) Wagner, C. D.; Zatko, D. A.; Raymond, R. H. *Anal. Chem.* **1980**, *52*, 1445.

(20) Ihara, H.; Kumashiro, Y.; Itoh, A.; Maeda, K. *Jpn. J. Appl. Phys.* **1973**, *12*, 1462.

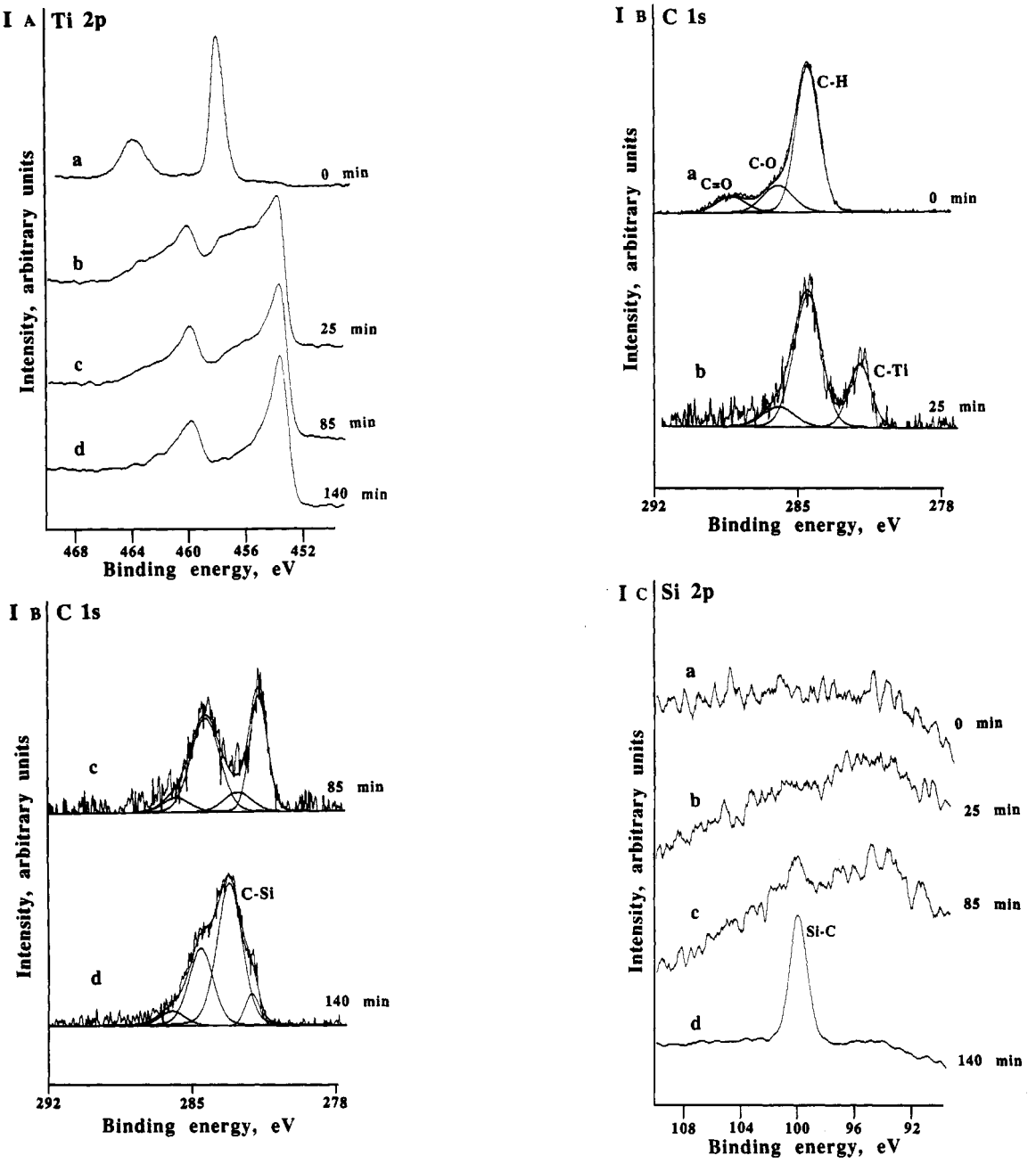

Figure 5. Line shape changes in the photoelectron spectra of the (I) titanium-coated SICABO fiber and (II) titanium-coated BORSIC fiber: (A) Ti 2p, (B) C 1s, and (C) Si 2p with increasing sputter time; (a) 0 min; (b) 25 min; (c) 85 min; (d) 140 min.

observed in the C 1s spectrum during argon ion sputtering for the Ti-SICABO and the Ti-BORSIC are summarized in Tables III and IV, respectively.

The presence of TiC in Ti-BORSIC is further supported by the Ti 2p spectrum of Ti-BORSIC, which shows a Ti $2p_{3/2}$ peak at 455.3 eV. This peak is assigned to TiC.[21] XPS did not reveal any silicon species on the surface of the Ti-SICABO and Ti-BORSIC fibers (Figure 5IC and 5IIC, respectively).

Differences are observed between the Si 2p spectra of the two coated fibers after argon ion sputtering. Ti-BORSIC shows a prominent SiC peak (Si 2p = 100.3 eV) and a silicide peak (Si 2p = 98.6 eV) only after a 4-min etch time. It is difficult to distinguish the silicides from Si 2p binding energies due to the small chemical shift among the various titanium silicides (see Table I) compared to the peak width of the Si 2p line. This has also been reported by Brunnix and co-workers.[22] The intensity of the silicide peak decreases on further etching. On the other hand, Ti-SICABO shows no Si 2p signal until only after 140 min of etch time. The Si species at this stage of depth profiling is SiC (Si 2p = 100.3 eV). A small broad shoulder is also seen at lower binding energy from the SiC peak which we attribute to small amounts of titanium silicides. Our earlier XRD work on these fibers revealed the presence of Ti_5Si_3 in Ti-SICABO and Ti_5Si_3 as well as TiSi in Ti-BORSIC.[2]

Argon ion etching for 25 min reveals the presence of titanium suboxides in both coated fibers. This is evident by the broad shoulder at the higher binding energy in the Ti 2p photoelectron spectrum.[23] Several differences are observed between the two coated fibers under study on argon ion etching. TiC begins to show in Ti–SICABO (Ti $2p_{3/2}$ = 455.0 eV and C 1s = 281.6 eV) while the peak corresponding to TiC in the C 1s spectrum of the Ti-BORSIC continues to grow in intensity.

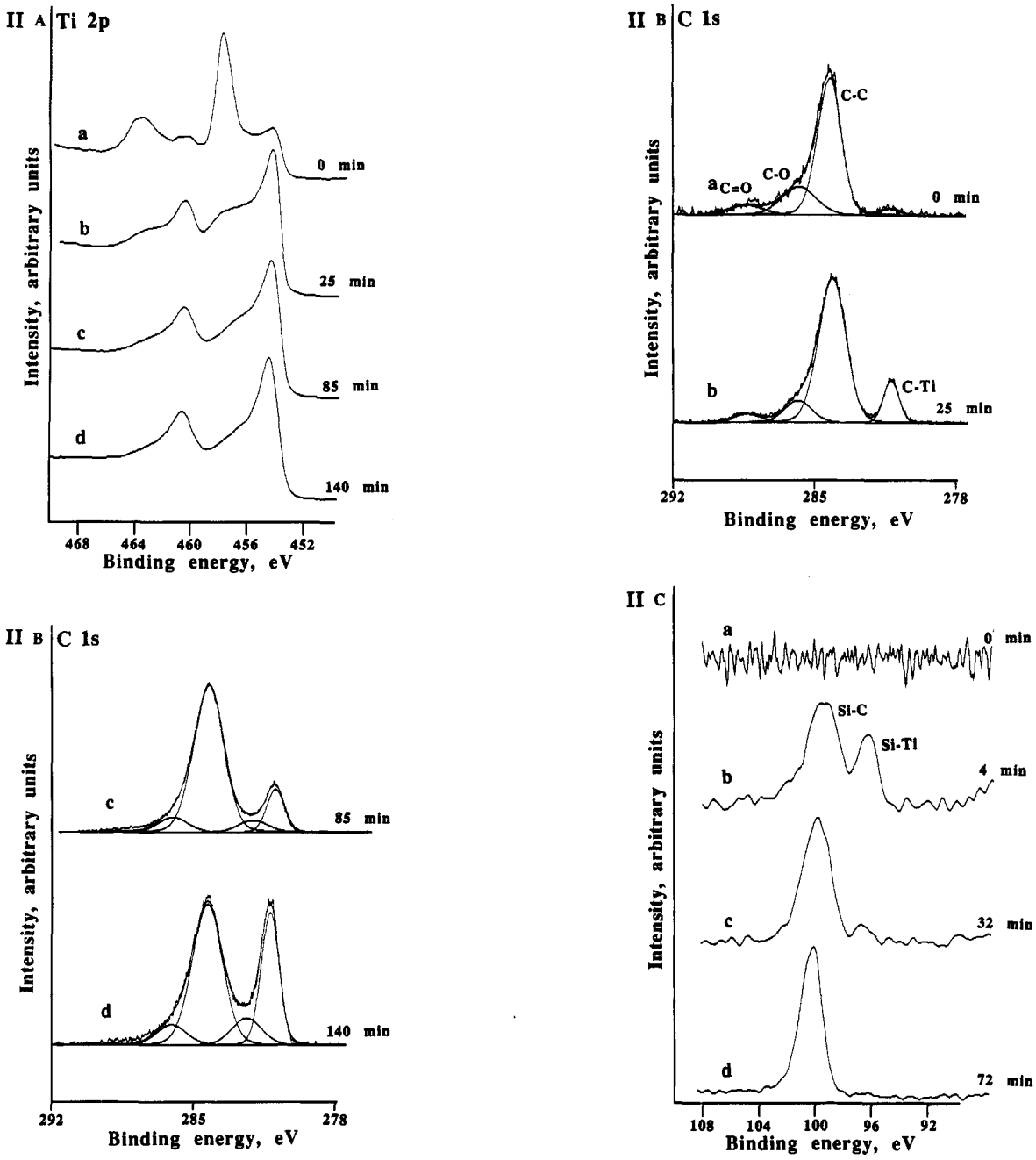

Figure 5. Continued.

Further argon ion sputtering decreases the amount of titanium suboxides in both coated fibers, as seen by the decrease in the intensity of the broad shoulder. This is accompanied by a shift of the main Ti 2p peak toward lower binding energy. After 140 min of argon ion sputtering, the Ti 2p peak was shifted down to 455.0 eV corresponding to TiC. The broadness of the Ti $2p_{3/2}$ peak of the Ti-BORSIC fiber (Figure 5IIC) indicates the presence of a mixture of titanium silicides, titanium carbide, and suboxides in the coating.[24]

(ii) AES results: The wide-scan AES spectrum for the as-coated fibers shows peaks due to C, Ti, and O. These wide scan AES spectra for Ti-SICABO and Ti-BORSIC are shown in Figure 6I and 6II, respectively. The presence of surface TiO_2 is again seen as a large O KLL peak in the wide AES spectra of both coated fibers. The surface oxide was removed on argon ion sputtering (seen as a decrease in the O KLL AES signal). The AES line changes observed in the Ti LMM spectrum on Ar^+ etching also suggest a surface composition of TiO_2 with a mixture of suboxides in the bulk of the Ti coating.

A very noticeable difference between the wide AES scans of the two coated fibers is the persistence of the Ti LMM signal in the Ti-BORSIC even after 72 min of argon ion sputtering (Figure 6IID). At this stage, the Ti LMM signal from the Ti-SICABO is almost at the noise level (Figure 6ID), indicating that the Ti coating has been sputtered through.

The expanded C KLL, Si LVV and Ti LMM Auger lines obtained for Ti-SICABO and Ti-BORSIC during the argon ion sputter depth profile are shown in greater detail in

(21) Sayers, C. N.; Armstrong N. R. *Surf. Sci.* **1978**, *77*, 301.
(22) Brunnix, E.; Thijssen, T. *Phillips J. Res.* **1988**, *43*, 1988.
(23) Ramquist, L.; Hamrin, K.; Johansson, G.; Gelius, U.; Nordling, C. *J. Phys. Chem. Solids* **1969**, *30*, 1849.
(24) Ramquist, L.; Ekstig, B.; Kallne, E.; Noreland, E.; Manne R. *J. Phys. Chem. Solids* **1969**, *30*, 1849.

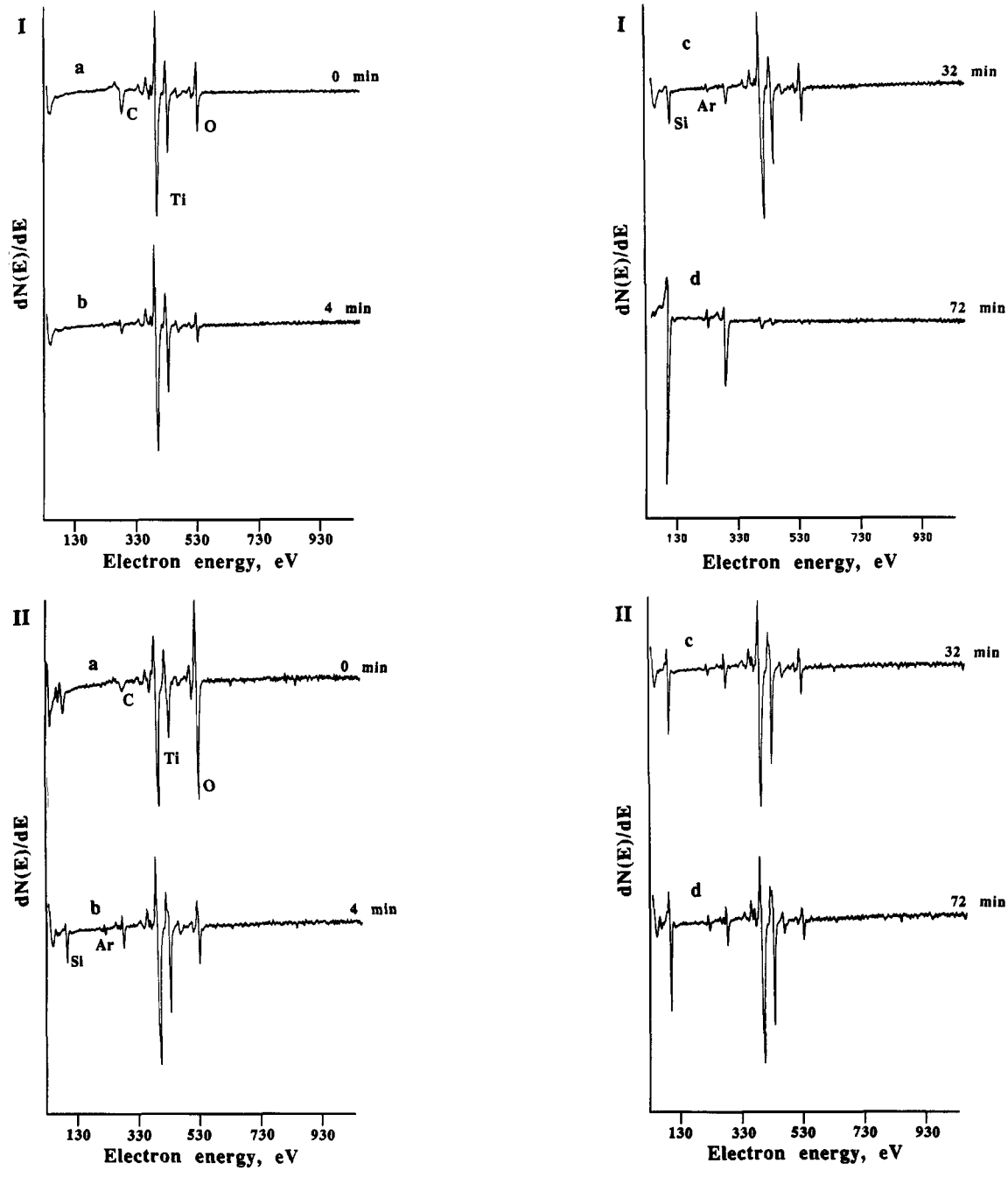

Figure 6. AES survey spectra of (I) titanium-coated SICABO fiber and (II) titanium-coated BORSIC fiber: (a) sample in the as-prepared state; (b) after 4-min argon ion sputter; (c) after 32-min argon ion sputter; (d) after 72-min argon ion sputter.

Figure 7I and 7II, respectively. Changes in the C KLL line shape during argon ion sputter indicate the presence of adventitious carbon on the surface of both coated fibers and carbidic carbon in the bulk of the coatings.

Differences are again observed between the C KLL Auger spectra of Ti-SICABO (Figure 7IA) and Ti-BORSIC (Figure 7IIA). The C KLL line shape for Ti-SICABO changes from that characteristic of adventitious carbon and surface hydrocarbons to that of TiC and finally to SiC (Figure 7IAb–e). The C KLL line feature after 32 min of etching shows two positive maximum peaks and negative maxima peak at 257, 268, and 272 eV. The line shape is similar to that of the TiC (100) surface.[21] At the point when the Si Auger peak appears, the positive peak at 261 eV, which is characteristic of β-SiC, increases in intensity and the intensities of the positive peaks at 257 and 268 eV decrease (Figure 7IAe). This trend continues until the carbon line shape becomes more and more characteristic of that of SiC after significant etching. A comparison of the line shape of the C peak at this point with that of the as-received SICABO fiber suggests that the depth profiling has reached the SICABO fiber and that the C peak observed at this stage is due to bulk SiC of the fiber.

In contrast, for the same total argon ion sputter time employed, the C KLL Auger line shape for the case of the Ti-BORSIC changes from that characteristic of adventitious carbon to that of TiC (Figure 7IIAb). The peak characteristic of SiC was not observed even after prolonged etching (Figure 7IIAd), and the C KLL line shape is still characteristic of TiC.

Differences between Ti-SICABO and again evident in the detailed AES Si LVV and C KLL spectra. The presence of titanium silicides is again evident from the spectral changes observed in the Si LVV signal for Ti-BORSIC.[25] The peak corresponding to titanium silicide

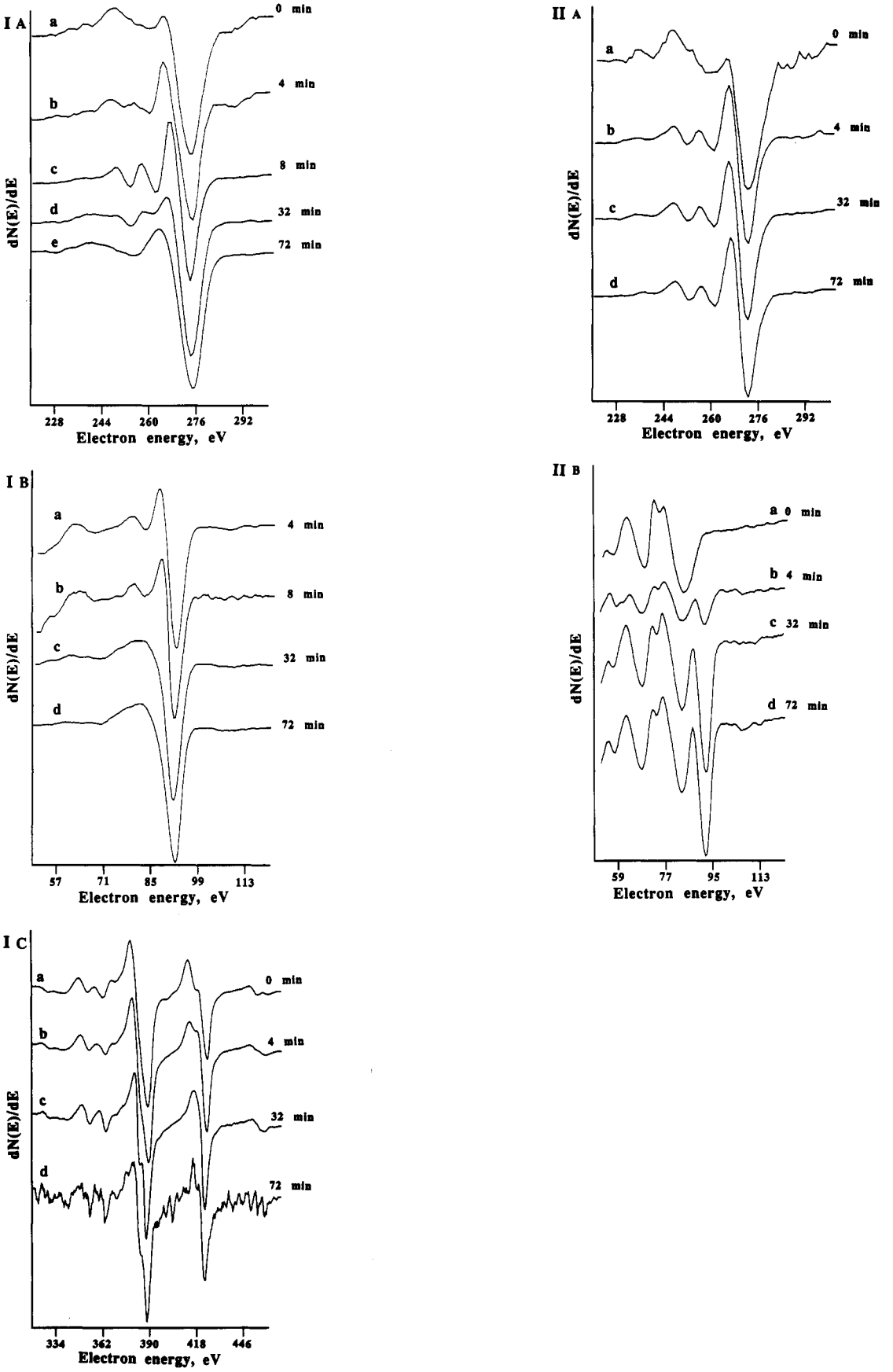

Figure 7. Auger line-shape changes in the spectra of the (I) titanium-coated SICABO fiber with increasing argon ion sputter time for: (A) C KLL Auger transition (a) 0 min, (b) 4 min, (c) 8 min, (d) 32 min, (e) 72 min; (B) Si LVV Auger transition (a) 4 min, (b) 8 min, (c) 32 min, (d) 72 min; (C) Ti LMM (a) 0 min, (b) 4 min, (c) 32 min, (d) 72 min as well as those of the (II) titanium-coated BORSIC fiber: (A) C KLL Auger transition (a) 0 min, (b) 4 min, (c) 8 min, (d) 32 min, (e) 72 min; (B) Si LVV Auger transition (a) 4 min, (b) 8 min, (c) 32 min, (d) 72 min.

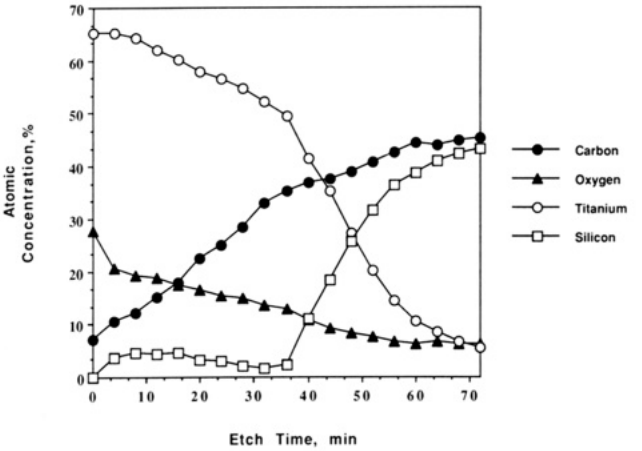

Figure 8. AES sputter depth profile for the titanium-coated SICABO fiber.

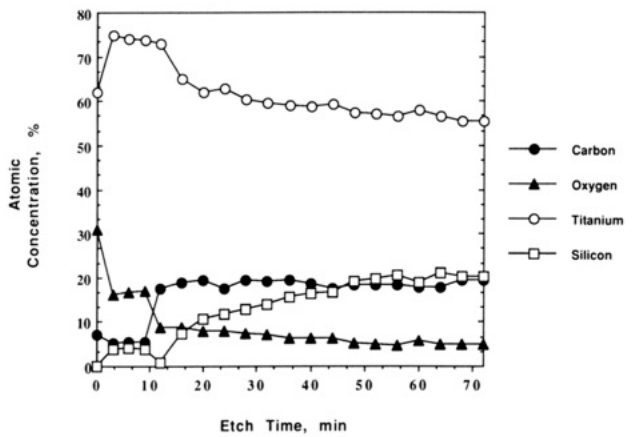

Figure 9. AES sputter depth profile for the titanium-coated BORSIC fiber.

is absent in the Si LVV signal of Ti-SICABO.

The AES depth profile results obtained for Ti-SICABO and Ti-BORSIC are shown in Figures 8 and 9, respectively. The atomic fractions of Si, C, Ti, and O are plotted as functions of sputter time. The sputter depth profile of Ti-SICABO shows that the O profile parallels that of the Ti profile until the matrix–fiber interface is reached. After this point the O profile levels off to the bulk O concentration of the SiC coating[2] and does not decrease further even though the Ti fraction decreases sharply. The AES depth profile result for the Ti-coated BORSIC fiber is different from that for the Ti-coated SICABO fiber in that the Ti concentration profile does not decrease even after etching well into the fiber. Thus the Ti diffusion zone in the Ti-BORSIC fiber is rather broad. The initial decrease in O concentration is due to the fact that surface TiO_2 is sputtered off during the first few minutes of argon ion etching. The O concentration then levels off to that of the bulk O content of the SiC coating.[2]

(iii) Scanning electron microscopy: Figure 10 shows the electron micrographs of the as-received and Ti-coated SICABO fibers. As Figure 10A shows, the surface of the as-received SICABO fiber has a nodular-like appearance. After Ti deposition, the surface of the Ti-coated SICABO fiber appears to consist of columns of titanium that grow upward from the fiber surface (Figure 10B). The cross section of the coated fiber, shown in Figure 10C, reveals that the thickness of the coating is about 1 μm. The surface morphology and thickness of the coating on the BORSIC fiber are similar to those observed for Ti-SICABO.

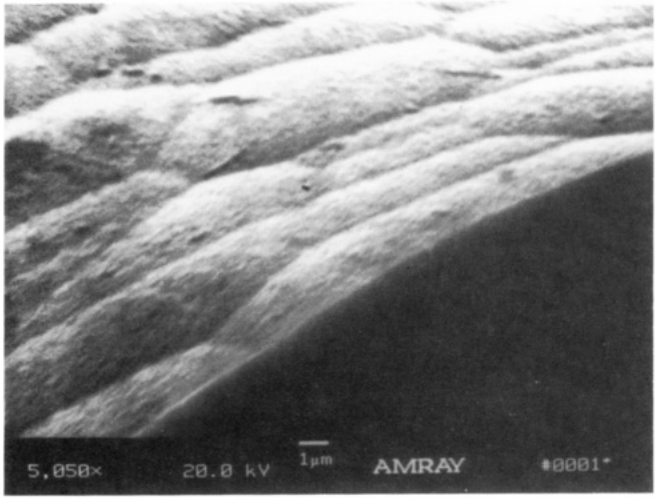

A

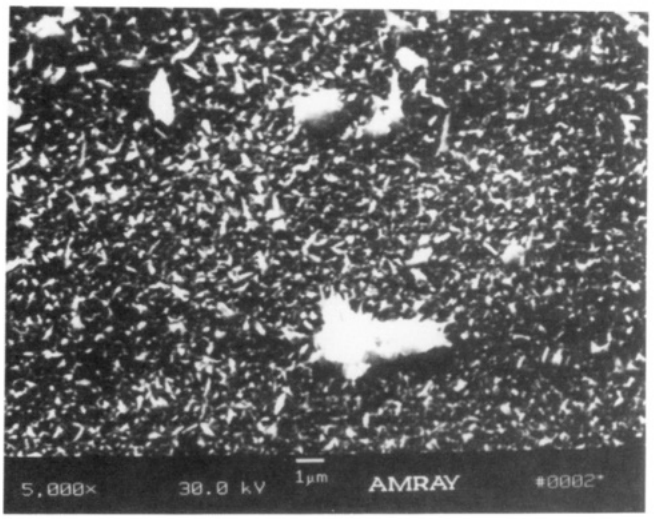

B

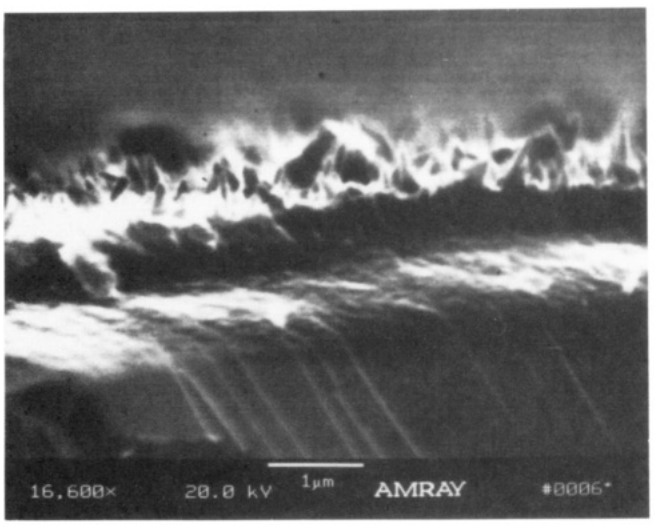

C

Figure 10. Scanning electron micrographs showing (A) the surface and end of the as-received SICABO fiber; (B) the surface of the CVD titanium-coated fiber and (C) the cross section of the coated fiber showing the titanium coating thickness.

(25) Galuska, A. A.; Wallace, W. O. *J. Vac. Sci. Technol.* **1989**, *7*, 9.

Discussion

In our earlier studies,[2] we reported that Ti-BORSIC fibers showed greater strength degradation than Ti-SICABO fibers when subjected to postdeposition treatments. We then set out to obtain information on the chemical composition of the Ti coating/fiber interface with a goal of understanding reaction processes occurring on the fiber surface as well as in the matrix–fiber interface when Ti is deposited onto the SiC-coated boron fibers.

The present study has shown that the surfaces of both Ti-SICABO and Ti-BORSIC fibers are rich in TiO_2. The TiO_2 coating probably resulted from the reaction of Ti with residual oxygen and absorbed water in the system. After argon ion etching of the surface, suboxide spectral components become visible. Prolonged sputtering of these fibers resulted in more than one Ti species being observed, although fully reduced Ti was never observed even after prolonged sputtering. However, argon ion bombardment of TiO_2 surfaces has been found to cause an apparent reduction of TiO_2 under the influence of high electron and ion beam power densities.[9,26-28] Thus, ion-etching depth profiles of TiO_2 surfaces must be interpreted carefully in order to understand this distribution of oxide species. From the present data, it is difficult to tell whether the Ti matrix actually possesses reduced oxide species immediately below the surface or whether these species were formed as a result of the sputtering process.

TiO_2, suboxides, TiC, and titanium silicides are present in the bulk of the Ti coating of both coated fibers. Tables III and IV show the presence of adventitious carbon contamination even after Ar^+ etching. It is therefore likely that TiC is formed from ion and electron bombardment. However, the presence of titanium silicides and carbides in these fibers were also confirmed by our earlier XRD results.[2,29] Thus the TiC observed by XPS and AES arises from the bulk of the coating as well as from contributions from artifacts of ion and electron bombardment. However, there are several differences in the extent and depth distribution to which these chemical species are present in the coatings of these two fibers.

The Ti-BORSIC fibers show the presence of TiC and titanium silicides throughout the entire Ti coating. In contrast, TiC was observed only at the matrix–fiber interface of the Ti-SICABO fiber. Another difference is that Ti-SICABO showed only small amounts of titanium silicides at the matrix–fiber interface, and titanium silicides were formed in much greater amounts throughout the Ti coating of the Ti-BORSIC fibers.

The AES sputter depth profiles for Ti-SICABO (Figure 8) and Ti-BORSIC (Figure 9) reveal that the Ti diffused deeper into the BORSIC fiber than the SICABO fiber. This is evident from the high atomic concentration of Ti throughout the depth profile of Ti-BORSIC. In the case of Ti-SICABO the Ti atomic concentration dropped dramatically on reaching the SiC coating of the fiber. This suggests that Ti has a more severe reaction with BORSIC than with SICABO, which results in Ti diffusing deep into the SiC coating of the BORSIC fiber and reacting with the SiC to form Ti silicides and carbides. In the case of the SICABO fiber, the Ti did not diffuse as far into the fiber. The reactive nature of Ti with Si, SiO_2, and SiC has been reported in the literature.[30-33]

We now need to explain the difference in the extent of chemical reaction between the Ti coating and the SICABO and BORSIC fibers and to propose reaction mechanisms for deposition of Ti onto SICABO and BORSIC fibers.

In an earlier study, we reported that the surface composition of SICABO fiber was richer in carbon than that of the BORSIC fiber.[34] Thus when Ti was deposited onto the SICABO fiber, there is an initial reaction of the Ti with the carbon-rich surface resulting in the formation of titanium carbide.

The formation of the TiC layer in the neighborhood of the SiC fiber results in a decrease of the reaction rate and the overall extent of reaction between Ti and SiC. At the deposition temperature of 1040 °C, reaction takes place at the gas/solid interface and Ti diffuses through the formed TiC layer.[35] The reaction rate is now determined by the diffusion rate of Ti through TiC. A 30-min chemical deposition of Ti apparently did not provide sufficient amounts of Ti to diffuse through the formed surface TiC layer and prevented significant reaction with SiC. A longer Ti deposition time results in the formation of titanium silicides with both fibers.[29]

In the case of Ti-BORSIC fiber, the lack of a carbon-rich surface results in the reaction of Ti with SiC and concomitant formation of TiC and Ti silicides. Ti diffuses into the SiC coating and continues to do so until the reaction zone grows thick enough and obstructs further reaction of Ti with SiC, because the supply of Ti to the SiC coating is decreased. Since TiC has the largest negative heat of formation compared to other phases,[36] it is preferentially formed. The resulting free Si then reacts with fresh Ti, forming Ti silicides.

Thus in SiC-coated boron fibers reinforced in a Ti matrix, the fiber and matrix react, resulting in fiber surface degradation. The extent of surface degradation may explain the degree of loss of strength of these fibers. Thus the difference in strength retention between Ti-SICABO and Ti-BORSIC fibers may be due to more severe matrix–fiber reactions with Ti-BORSIC fibers than Ti-SICABO fibers, as shown in the present study. The carbon-rich surface protects the SiC coating of SICABO fibers from detrimental chemical reactions with the Ti coating.

Future work on the development of a SiC-coated boron fiber with a reinforced Ti matrix is underway. An improvement of tensile strength could be achieved if one can minimize fiber surface degradation. Covering the SiC-coated boron fibers with TiC or Ti silicides before introducing them in the Ti matrix might be successful procedures for improvement of these composites.

Conclusions

XPS and AES studies have shown that chemical vapor deposition of Ti onto SICABO and BORSIC fibers at 1040 °C results in the reaction of Ti with the fiber surface. In the case of SICABO fiber, the carbon-rich surface results in the formation of a protective titanium carbide layer, thus impeding the diffusion of Ti into the SiC coating of the fiber. In the case of BORSIC fiber, in which the

(26) Chung, Y. W.; Lo, W. J.; Somorjai, G. A. *Surf. Sci.* **1977**, *64*, 588.
(27) Lo, W. J.; Chung, Y. W.; Somorjai, G. A. *Surf. Sci.* **1978**, *71*, 71.
(28) Khotek, K. L.; Houston, J. F. *Phys. Rev.* **1977**, *B15*, 4580.
(29) Hwan, L.; Tan, B. J.; Suib, S. L.; Galasso, F., manuscript in preparation.
(30) Hasegawa, S.; Nakamura, S. *Surf. Sci.* **1988**, *206*, L851.
(31) Singh, A.; Khokle, W. S. *Microelectron. J.* **1989**, *20*, 27.
(32) Bute, R.; Rubloff, G. W.; Tan, T. Y.; Ho, P. S. *Phys. Rev.* **1984**, *B30*, 5421.
(33) Quenisset, C.; Naslain, R.; Demonay, P. *Surf. Interfac. Anal.* **1988**, *13*, 123.
(34) Hwan, L.; Suib, S.; Galasso, F. *J. Am. Ceram. Soc.* **1989**, *72*, 1259.
(35) Aggour, L.; Fitzer, E.; Schlichting, J. *Proc. CVD 5th. Int. Conf.*; Blocher, J. M., Hintermann, H. E., Hall, L. H., Eds.; The Electrochem. Society: Princeton, NJ, 1975.
(36) *CRC Handbook of Chemistry and Physics*, 64th ed.; Weast R. C., Astle, M. J., Beyer, W. H., Eds.; CRC Press: Boca Raton, FL, 1983.

surface is not carbon rich, decomposition of SiC occurs and titanium silicides and titanium carbide are formed.

Acknowledgment. This work was supported by the State of Connecticut, Department of Higher Education, High Technology Grant Number 42.

Registry No. Ti, 7440-32-6; B, 7440-42-8; SiC, 409-21-2; TiC, 12070-08-5; SiO_2, 7631-86-9; TiO_2, 13463-67-7; titanium silicides, 12738-91-9.

Additions and Corrections

1989, Volume 1.

Duncan W. Bruce,* David A. Dunmur, Peter M. Maitlis, Peter Styring, Miguel A. Esteruelas, Luis A. Oro, M. Blanca Ros, José-Luis Serrano, and Eduardo Sola: Nematic Phases in Ionic Melts: Mesogenic Ionic Complexes of Silver(I).

Page 479. In the paper, we reported the phase behavior of $[Ag(4\text{-}OPhVPy)_2][DOS]$ incorrectly. The correct behavior is described according to

$K\text{-}S_A$	147 °C	ΔH = 32.68 J g^{-1}	$\Delta S_m/R$ = 8.1
$S_A\text{-}N$	166 °C	ΔH = 0.7 J g^{-1}	$\Delta S_m/R$ = 0.6
N–I	178 °C	ΔH = 0.2 J g^{-1}	$\Delta S_m/R$ = 0.07

Further, the mesophase does not change on treatment of the sample with wet acetone. Simply the strongly homeotropic texture of the S_A phase is replaced by the more readily identifiable focal conic texture.

1991, Volume 3.

David K. Liu,* Roger J. Chin, and Angela L. Lai: Photochemical Vapor Deposition of Iron–Cobalt Thin Films: Wavelength and Temperature Control of Film Compositions.

Page 14. In the second paragraph, sixth sentence, the units for saturation moment should be μ_B/mol.